

Janos Toth¹, Tibor Bodi², Peter Szucs¹, Faruk Civan³

¹ *Research Institute of Applied Chemistry, University of Miskolc,*

² *Petroleum Engineering Department, University of Miskolc,*

³ *School of Petroleum and Geological Engineering,
The University of Oklahoma,*

LINEAR EQUATIONS DERIVED FROM LABORATORY EXPERIMENTS TO DESCRIBE IMMISCIBLE DISPLACEMENT

An accurate analytical interpretation method to determine the Leverett-function (f_w) and its derivative (f_w') from immiscible displacement data in core plugs is presented. Linear equations are developed to describe the displacement processes occurring before and after breakthrough. A quadratic function is introduced to represent the saturation distribution along the cores. The relationships derived in this study can be used for analysis of core tests involving constant injection rates and constant pressure differences. The applicability, practicality, and accuracy of the new analytical method are verified by means of the experimental data obtained in the present study and by those reported in the literature.

INTRODUCTION

The analysis of the displacement processes of immiscible fluids (water, oil, gas) in porous core plugs essentially requires (1) the relationships between the volumes of the injected and produced fluids and (2) the injected or displaced fluid saturation distributions along the core plug as a function of time.

The theoretical descriptions of the immiscible fluid displacement have been presented by Leverett [1], Buckley and Leverett [2] and Welge [3]. Also, various attempts [4]-[8] have been made to develop methods for interpretation of the laboratory core flow tests and determining the capillary pressure and/or relative permeability curves. The data of the injected and produced fluid volumes after breakthrough in immiscible displacements have been used for the estimation of the petrophysical properties by empirical correlations [9],[10], by discrete means [Ucan et al., 15], graphical procedures [11] and analytical means [Shen and Ruth, 14]. However, most of these methods are computationally tedious.

The study by Ucan et al. [15] has indicated that uniqueness in the interpretation of displacement data can only be achieved by facilitating both the internal and external fluid measurements. Therefore, the determination of the local water or oil saturations at different points along the core plug is especially important for accurate interpretation of laboratory experiments. However, the direct measurement techniques resorted for this purpose, such as CT scanning, gamma-ray attenuation and NMR imaging, are expensive and time consuming.

This paper presents a new practical method, which alleviates the aforementioned problems. The present study is restricted to the presence of two mobile fluids. A third type of fluid might be present in the pores, but it is considered stationary under the ap-

plied pressure gradient. Fluid displacement tests can be carried out with a constant flow rate of the injected fluid, then the pressure difference across the core plug changes, or with a constant pressure difference applied across the core plug, then the flow rate of the injected fluid varies. Until the breakthrough, the fluid injected into the core plug progresses ahead inside the core, but only the displaced fluid present in the core is produced at the outlet face. After the breakthrough, the injected and displaced fluids are simultaneously produced at the outlet face. Therefore, the fluid displacements before and after the breakthrough of the injected fluid are analysed as two separate problems. The practical parity relationships necessary for analysis and interpretation of the immiscible fluid displacement in laboratory cores are formulated and verified by experimental data.

FORMULATION

Consider the one-dimensional horizontal flow of two immiscible fluids through a porous rock core plug. The physical properties of the fluids and the rock are assumed constant. The present laboratory experiments have used cores with 5 to 95 cm in length and 2 to 4 cm in diameter which were extracted from natural or artificial rocks. Although some inhomogeneity and heterogeneity may exist in the natural and artificial rocks used in the core flow tests, the formulation is carried out assuming homogeneous cores, because the method presented here does not require the local saturation values and the objective is to derive the parity relationship between the inlet and outlet flow conditions of a core plug during immiscible fluid displacement. Therefore, the internal details of the flow pattern is not of a concern here. The displaced and injected fluids are denoted by the subscript k and d , respectively.

Assume that the rock is initially ($t=0$) fully saturated with the wetting fluid and there is no irreducible non-wetting fluid present. Thus, the irreducible non-wetting fluid saturation is $S_{d0} = 0$ and the wetting fluid saturation is $S_{k0}=1$. The non-wetting fluid is injected into the core at a flow rate of q_{di} . Then, the cumulative volume of the injected fluid is given by:

$$V_i = \int_0^t q_{di} dt . \quad (1)$$

Let q_k and q_d represent the effluent flow rates of the displaced and injected fluids at the core outlet, respectively. Then, the cumulative effluent volumes of the displaced and injected fluids are given, respectively, by:

$$V_k = \int_0^t q_k dt ; \quad (2)$$

$$V_d = \int_0^t q_d dt . \quad (3)$$

Assuming that the fluids are incompressible under the applied pressure conditions of the experimental core flow tests, the overall volumetric balance of the fluids over the core plug after the breakthrough of the injected fluid is given by:

$$V_i = V_k + V_d . \quad (4)$$

Similarly, the following equation can be written for the flow rates:

$$q_{di} = q_k + q_d . \quad (5)$$

The effluent production rate and cumulative volume of the injected fluid are zero until the breakthrough. Therefore, before and at the breakthrough time , $t=t_a$, Eqs. 4 and 5 simplify, respectively as:

$$V_{ia} = V_{ka} ; \quad (6)$$

$$q_{di} = q_{ka} \mathcal{Q} . \quad (7)$$

After the breakthrough, the fractional flows of the produced fluids at the effluent side of the core plug are given, respectively, by:

$$f_k = \frac{q_k}{q_{di}} ; \quad (8)$$

$$f_d = \frac{q_d}{q_{di}} . \quad (9)$$

If capillary effects are negligible, consider Welge's [3] equation given by:

$$\frac{df_d}{dS_d} = f'_d = \frac{1-f_d}{\overline{S_d} - S_d} = \frac{f_k}{(\overline{S_d} - S_{d0}) - (S_d - S_{d0})} = \frac{1}{\frac{V_i}{V_p}} \quad (10)$$

from which the following expression is obtained:

$$\frac{V_i}{V_p} = \frac{(\overline{S_d} - S_{d0}) - (S_d - S_{d0})}{f_k} , \quad (11)$$

$\overline{S_d}$ and V_p denote the core length average saturation of the injected fluid and the pore volume of the core, respectively.

Invoking Eqs. 1 and 2 into Eq. 8 yields:

$$f_k = \frac{dV_k}{dV_i} . \quad (12)$$

In addition, a volume balance between the injected and displaced fluids over the core leads to the following equation:

$$(\overline{S_d} - S_{d0}) = \frac{V_k}{V_p} . \quad (13)$$

Therefore, substituting Eqs. 12 and 13 into Eq. 11, yields the following expression:

$$\frac{V_i}{V_p} = \frac{\frac{V_k}{V_p} - (S_d - S_{d0})}{\frac{dV_k}{dV_i}} . \quad (14)$$

The relationships given by Eqs. A20 and A21 in the appendix can be combined to yield:

$$(S_d - S_{d0}) = b \left(\overline{S_d} - S_{d0} \right)^2 = b \left(\frac{V_k}{V_p} \right)^2 , \quad (15)$$

where „b” is an integration constant as defined in the appendix.

Thus, substituting Eq. 15 into Eq. 14, and then considering that the pore volume V_p remains constant and separating the variables, a differential equation in the following form can be obtained:

$$\frac{d\left(\frac{V_i}{V_p}\right)}{\frac{V_i}{V_p}} = \frac{d\left(\frac{V_k}{V_p}\right)}{\frac{V_k}{V_p} \left[1 - b\left(\frac{V_k}{V_p}\right)\right]} \quad (16)$$

The general solution of Eq. 16 yields a linear expression as:

$$\frac{V_i}{V_k} = a + b \frac{V_i}{V_p}, \quad (17)$$

where „a” is an integration constant, V_i/V_p is the independent variable, and V_i/V_k is the dependent variable. Applying Eq. 6 at the breakthrough time ($t=t_a$), Eq. 17 simplifies to:

$$\frac{V_i}{V_p} \Big|_a = \frac{1-a}{b} \quad (18)$$

In addition, the following equation can also be written based on Eq. 11:

$$\frac{V_{ia}}{V_p} = \frac{V_{ka}}{V_p} = \overline{S}_{df} - S_{d0} = \frac{1-a}{b}, \quad (19)$$

where \overline{S}_{df} is the average saturation of the injected fluid at breakthrough. Thus, substituting Eq. 19 into Eq. 15 yields:

$$S_{df} - S_{d0} = \frac{(1-a)^2}{b}. \quad (20)$$

Next consider Welge's [3] equation given by:

$$f'_{df} = \frac{f_{df}}{S_{df} - S_{d0}} = \frac{I}{S_{df} - S_{d0}}, \quad (21)$$

where the subscript, f, denotes to the shock front. Therefore, substituting Eqs. 19 and 20 into Eq. 21 results in the following expression for the integration constant, „a”:

$$a = 1 - f_{df} = f_{kf}. \quad (22)$$

According to Eq. 22, the integration constant, „a”, is equal to the fractional flow of the displaced fluid at the breakthrough time.

The integration constant, „b”, can be determined by considering the condition at the infinite volume of the injection fluid throughput ($t \rightarrow \infty$, and $V_i \rightarrow \infty$). At this state, the displaced fluid saturation reaches its minimum value, i.e. the irreducible saturation $S_{k \min} = S_{km}$, and the injected fluid saturation reaches its maximum value. Thus, the limit of Eq. 17 can be expressed as:

$$\frac{V_k}{V_p} \Big|_{\frac{V_i \rightarrow \infty}{V_p}} = \frac{1}{b} = \overline{S}_{d \max} - S_{d0} = S_{d \max} - S_{d0}. \quad (23)$$

Substituting Eqs. 22 and 23 for the integration constants, „a” and „b”, into Eq. 17 gives a linear equation between $\frac{V_i}{V_k}$ and $\frac{V_i}{V_p}$ as:

$$\frac{V_i}{V_k} = (1 - f_{df}) + \frac{1}{[S_{d \max} - S_{d0}]} \frac{V_i}{V_p}. \quad (24)$$

Eliminating the integration constant, „b”, between Eqs. 15 and 23 leads to:

$$\left(\overline{S_d} - S_{d0}\right) = \sqrt{\left(S_d - S_{d0}\right)\left(S_{d \max} - S_{d0}\right)}. \quad (25)$$

This equation expresses the average saturation increment of the injected fluid as the geometric mean of the injected fluid saturation increments at the inlet and outlet faces of the core plug.

In the next section, Eqs. 24 and 25 are applied to interpret the results of the laboratory displacement experiments conducted in two steps: (1) Oil injection into a water saturated core having initially no irreducible oil available and then (2) water injection into the previously oil injected core which may or not have attained the irreducible water saturation state.

At the first step, an air-dry rock core sample is placed into the core holder. The core is fully saturated by water ($S_w=1$) and the pore volume (V_p) of the core is determined. Then, the water is displaced by injecting oil into the core plug. For the present oil/water system, Eqs. 24 and 25 can be rewritten, respectively, as the following, by replacing $d \rightarrow o$ because the injected fluid is oil and $k \rightarrow w$ because the displaced fluid is water and by considering that the initial the oil saturation in the rock is zero ($S_{o0}=0.0$).

$$\frac{N_i}{W_p} = \left(1 - f_{of}\right) + \frac{1}{S_{o \max}} \frac{N_i}{V_p}, \quad (26)$$

where N_i and W_p are the cumulative volumes of the oil injected at the core inlet and the water produced at the core outlet sides, respectively. The core length average oil saturation is given by:

$$\overline{S_o} = \sqrt{S_o S_{o \max}}. \quad (27)$$

Following the injection of oil over a sufficiently long period of time, the rock attains the irreducible water saturation $S_{w0} = S_{wi} = 1 - S_{o \max}$ and the oil saturation reaches its maximum $S_{o0} = S_{o \max}$. Then, the oil is displaced by injecting water. In this case, Eqs. 24 and 25 can be rewritten, respectively, as the following by substituting $d \rightarrow w$ because the injected fluid is water and $k \rightarrow o$ because the displaced fluid is oil:

$$\frac{W_i}{N_p} = \left(1 - f_{wf}\right) + \frac{1}{\left(S_{w \max} - S_{wi}\right)} \frac{W_i}{V_p}; \quad (28)$$

$$\left(\overline{S_w} - S_{wi}\right) = \sqrt{\left(S_w - S_{wi}\right)\left(S_{w \max} - S_{wi}\right)}. \quad (29)$$

The equations presented above are valid for both the $q_{di}=\text{constant}$ and $\Delta p = \text{constant}$ cases.

APPLICATIONS AND VERIFICATION

The schematic drawing of the equipment used in the laboratory experiments is shown in Fig. 1. Essentially it consists of the water and oil containers and a Hassler-type coreholder. The outlet face is open to the atmospheric pressure. Thus, during the displacement process, the inlet face pressure is the differential gauge pressure. The volumes of the produced fluids (oil and water) are measured as a function of time using graduated cylinders. Water or oil injection is accomplished by applying the N_2 gas at constant pressure. The parameters of the cores used in the experiments are summarised in Table 1. The results of the experimental displacement processes conducted in the present study are presented in Table 2. The processed parameters of the displacement data extracted from the literature are calculated using Eq. 17 are also given in Table 2. The measured data of typical experiments are plotted in

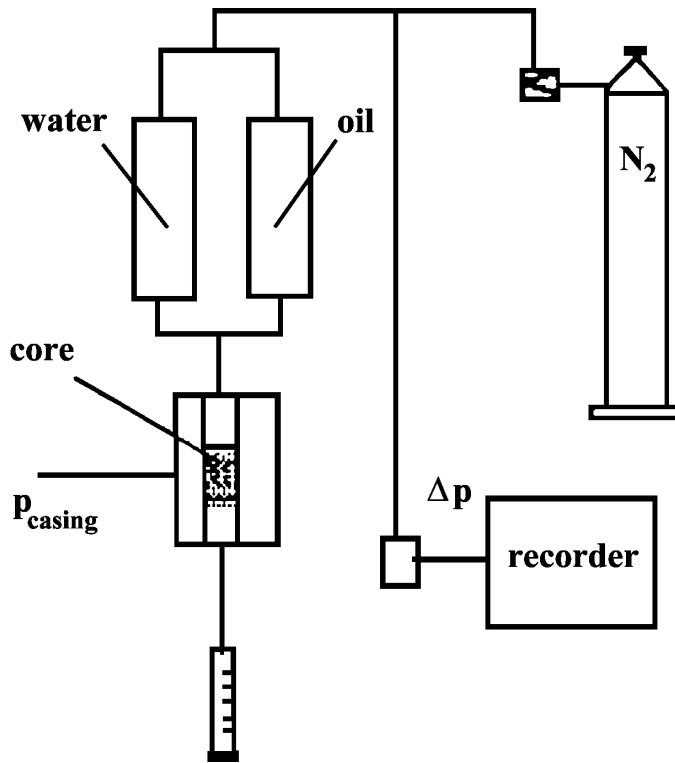


Fig. 1. The schematic of the equipment used for the displacement experiments

Fig. 2.

As indicated by Fig. 2, the plot of the experimental data yields straight lines, confirming the validity of the linear relationship between the volume of injected oil and produced water as implied by Eq. 26 for the water saturated rock displaced by oil. From the conditions of the above described theoretical derivation and experimental results the following conclusions are drawn:

1. In case of water wet rock, $S_{o_{max}} < 1$. Therefore, $b > 1$. The closer the b parameter is to the unity, the greater the maximum oil saturation and the less the irreducible water saturation are. These are the characteristics of the high porosity rocks. Conversely, the greater the b value, the smaller $S_{o_{max}}$ and the greater S_{wi} are in low porosity rocks.

2. The parameter a varies in the range of $0 < a < 1$ because after the breakthrough of the oil front, the value of the fractional oil varies in the $0 < f_{of} < 1$ range, and $f_{of} = 1 - a$ according to Eq. 22. Generally, the value of a is near the lower end of the (0-1) interval, because water can be displaced by oil with good efficiency.

Table 1. The parameters of the cores used in the displacement experiment and calculation

Cores	L cm	d cm	A cm ²	V _p cm ³	f	k _w (S _w =1) D	S _{wi}	S _{oi}	Displ. type
Jones-Roszelle (Table 1.) [11]	12.71	3.81	11.40	31.14	0.2150	0.0354	0.3500	0.6500	q _{wi}
Jones-Roszelle (Table 3.) [11]	12.71	3.81	11.40	31.14	0.2150	0.0354	0.3500	0.6500	Δp
Odeh-Dotson (Table 2.) [8]	7.62	2.54	5.07	8.76	0.2270	0.0251	0.4190	0.5810	q _{oi}
Odeh-Dotson (Table 3.) [8]	7.62	2.54	5.07	8.76	0.2270	0.0251	0.4190	0.5810	q _{oi}
Odeh-Dotson (Table 4.) [8]	7.62	2.54	5.07	8.76	0.2270	0.0251	0.4190	0.5810	q _{oi}
Odeh-Dotson (Table 5.) [8]	7.62	2.54	5.07	8.76	0.2270	0.0251	0.4190	0.5810	q _{oi}
Batycky-M-H-F Sec. displ. [10]	25.20	-	20.43	110.69	0.2150	0.4760	0.5700	0.4300	q _{oi}
Batycky-M-H-F Imbibition [10]	25.20	-	20.43	110.69	0.2150	0.4760	0.4760	0.5240	q _{wi}
Tóth János Kőolaj és Földgáz [7]	5.67	-	11.95	12.80	0.1890	0.0226	1.0000	0.0000	Δp
D-1 core Displacement	5.50	4.00	12.57	16.97	0.2455	0.2304	1.0000	0.0000	Δp
D-1 core Imbibition	5.50	4.00	12.57	16.97	0.2455	0.2304	0.2609	0.7391	Δp
D-2 core Imbibition	5.50	4.00	12.57	15.85	0.2294	-	0.2865	0.7135	Δp
D-5 core Imbibition	7.94	4.00	12.57	23.50	0.2355	0.2107	0.3040	0.2865	Δp
B core Displacement	5.50	4.00	12.57	29.95	0.4333	1.9320	1.0000	0.0000	Δp
B core Imbibition	5.50	4.00	12.57	29.95	0.4333	1.9320	0.4285	0.5715	Δp

Displacement type:

q_{wi} - constant water injection rate

q_{oi} - constant oil injection rate

Δp - constant differential pressure

Table 1.(continued) The parameters of the cores used in the displacement experiment and calculation

Cores	L cm	d cm	A cm ²	V _p cm ³	f	k _w (S _w =1) D	S _{wi}	S _{oi}	Displ. type
T-1 core Displacement	5.75	4.00	12.57	10.33	0.1430	0.0065	1.0000	0.0000	Δp
T-1 core Imbibition	5.75	4.00	12.57	10.33	0.1430	0.0065	0.5414	0.4586	Δp
T-2 core Displacement	5.81	4.02	12.57	11.96	0.1638	0.0094	1.0000	0.0000	Δp
T-2 core Imbibition	5.81	4.02	12.57	11.96	0.1638	0.0094	0.4484	0.5516	Δp
IV- core Imbibition	59.70	-	8.16	101.72	0.2088	0.1321	0.1642	0.8358	q _{wi}
V- core Imbibition	59.40	-	8.58	111.00	0.2178	0.2385	0.2523	0.7477	q _{wi}
VI- core Imbibition	59.00	-	8.62	87.98	0.1730	0.1730	0.2841	0.7159	q _{wi}
I- core Imbibition	59.80	-	9.80	96.99	0.1655	0.2013	0.1113	0.8887	q _{wi}
II- core Imbibition	59.70	-	8.86	85.48	0.1616	0.1729	0.3217	0.6783	q _{wi}
III- core Imbibition	59.30	-	9.04	97.08	0.1811	0.1941	0.3454	0.6546	q _{wi}
1- core Imbibition	95.00	-	5.47	123.62	0.2379	0.1256	0.4256	0.5744	Δp
2- core Imbibition	95.80	-	5.85	111.02	0.1981	0.0459	0.0180	0.9820	Δp
3- core Imbibition	95.00	-	5.85	106.93	0.1924	0.1055	0.0294	0.9706	Δp
4- core Imbibition	95.00	-	5.64	97.09	0.1812	0.1695	0.0474	0.9526	Δp
5- core Imbibition	95.00	-	5.15	107.98	0.2207	0.2511	0.0741	0.9259	Δp
6- core Imbibition	80.00	-	4.58	82.99	0.2265	0.0014	0.2048	0.7952	Δp
7- core Imbibition	80.00	-	4.60	86.00	0.2337	0.0146	0.3488	0.6512	Δp
8- core Imbibition	95.00	-	5.21	108.00	0.2182	0.1220	0.1019	0.8981	Δp

Displacement type:

q_{wi} - constant water injection rate

q_{oi} - constant oil injection rate

Δp - constant differential pressure

Table 2. The results obtained from the displacement data

Cores	μ_w/μ_{wp}	N_w/N_p	N_w/N_p	q_w/A cm/min	q_w/A cm/min	q_w/A cm/min	Δp bar	a	b	Regression Coefficient
Jones-Roszelle (Table 1.) [11]	10.7732	-	10.0000	-	-	0.1169	-	0.40422	2.98837	0.99998
Jones-Roszelle (Table 3.) [11]	10.7732	-	8.8950	-	-	-	6.8966	0.39715	2.98927	0.99996
Odeh-Dotson (Table 2.) [8]	3.2473	2.0080	-	0.09868	-	-	-	0.46705	3.99469	0.99969
Odeh-Dotson (Table 3.) [8]	3.2473	2.0171	-	0.06907	-	-	-	0.58755	4.04093	0.99847
Odeh-Dotson (Table 4.) [8]	3.2473	2.0170	-	0.02960	-	-	-	0.55013	4.17404	0.99955
Odeh-Dotson (Table 5.) [8]	3.2473	2.0171	-	0.00987	-	-	-	0.41279	4.20000	0.99973
Batycky-M-H-F Sec. displ. [10]	0.5642	3.7864	-	0.01619	-	-	-	0.82770	5.96964	0.99952
Batycky-M-H-F Imbibition [10]	0.5642	-	69.2000	-	-	0.00973	-	0.04749	6.58990	0.99989
Tóth János Kőolaj és Földgáz [7]	2.1298	-	21.9112	-	-	-	3.5000	0.58915	1.49294	0.99989
D-1 core Displacement	1.5000	5.7075	-	-	-	-	0.1267	0.13156	1.35305	0.99995
D-1 core Imbibition	1.5000	-	3.9505	-	-	-	0.064-0.035	0.07940	1.66223	0.99995
D-2 core Imbibition	1.5000	-	6.4353	-	-	-	0.096-0.073	0.13324	2.10229	0.99999
D-5 core Imbibition	1.5000	-	6.3837	-	-	-	-	0.38132	2.32805	0.99981
B core Displacement	1.5000	5.3224	-	-	-	-	0.045-0.015	0.19850	1.74451	0.99992
B core Imbibition	1.5000	-	-	-	-	-	-	0.12958	1.99784	0.99914

Table 2. (Continued) The results obtained from the displacement data

Cores	μ_o/μ_w	N_o/N_p	N_w/N_p	q_o/A cm/min	q_w/A cm/min	Δp bar	a	b	Regression Coefficient
T-1 core Displacement	1.5000	2.5944		$0.032378 \cdot t^{0.98574}$	-	0.3346	0.10445	1.84722	0.99991
T-1 core Imbibition	1.5000	-	0.7744	-	$0.0052526 \cdot t^{1.06558}$	0.4159	0.16577	2.97604	0.99728
T-2 core Displacement	1.5000	4.7024		$0.017858 \cdot t^{1.136724}$	-	-	0.14066	2.22991	0.99993
T-2 core Imbibition	1.5000	-	2.1815	-	$0.019785 \cdot t^{1.035491}$	0.2633	0.11496	3.19048	0.99973
IV- core Imbibition	6.4599	-	1.9764	-	0.01593	-	0.47710	1.98984	0.99980
V- core Imbibition	6.4599	-	1.7207	-	0.01166	-	0.32090	2.35128	0.99994
VI- core Imbibition	6.4599	-	1.9663	-	0.01160	-	0.38707	2.39268	0.99987
I- core Imbibition	6.9229	-	-	-	0.01531	-	0.23718	1.43739	-
II- core Imbibition	6.7088	-	-	-	0.01467	-	0.37197	3.07338	-
III- core Imbibition	6.7088	-	-	-	0.01438	-	0.31676	3.27673	-
1- core Imbibition	-	-	1.8163	-	-	-	0.19094	2.00667	0.99995
2- core Imbibition	-	-	1.5222	-	-	-	0.26669	1.76432	0.99973
3- core Imbibition	-	-	1.8284	-	-	-	0.33664	1.38184	0.99747
4- core Imbibition	-	-	1.9364	-	-	-	0.28068	1.25295	0.99462
5- core Imbibition	-	-	2.0004	-	-	-	0.29838	1.57004	0.99974
6- core Imbibition	-	-	1.3797	-	-	-	0.11595	1.94599	0.99995
7- core Imbibition	-	-	2.1104	-	-	-	0.21915	2.02063	0.99999
8- core Imbibition	-	-	2.5954	-	-	-	0.46564	1.17653	0.99832

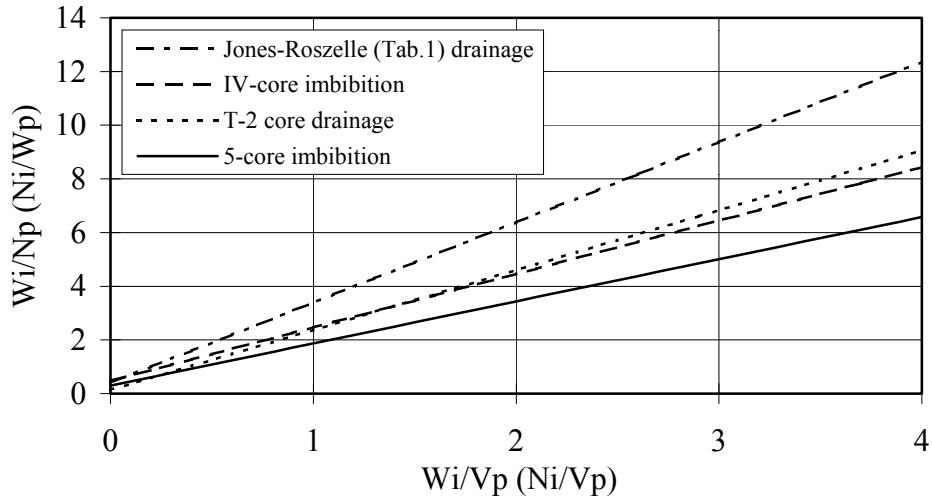


Fig. 2. The plots of typical displacement data according to the present theory.

The water displacement follows the above described oil displacement process. It is possible that the $S_{w0} > S_{wi}$ state can be reached instead of the state $S_{wi} = 1 - S_{omax}$ assumed in the above formulation. Thus, some modifications are necessary to take into account the amount of water $V_p(S_{w0} - S_{wi}) = V_{w0}$. Again, the plots of data display straight line trend as shown in Fig. 2 confirming the validity of the linear Eq. 28 for the water displacement. In this case, the following observations are made:

1. As $b = (S_{wmax} - S_{w0})^{-1}$ according to Eq. 23, therefore $b > 1$, because $S_{wmax} < 1$ and $S_{w0} > 0$. The value of b is smaller in the water displacement than the oil displacement. It was also observed that $(S_{wmax} - S_{w0}) < S_{omax}$.

2. The parameter, a , is less than 1 because $f_{wf} = 1 - a$ according to Eq. 22 and $0 \leq f_{wf} \leq 1$. The value of the parameter, a , associated with the water displacement is greater than that of the oil displacement, because the water, which has a lower viscosity, displaces the oil with a poor efficiency.

CONCLUSIONS

Both the data extracted from the literature and those measured in the present study have verified that the linear type relations indicated by Eq. 26 and 28 are valid and accurately describe the immiscible displacement processes conducted at constant injection flow rates or constant pressure differences across the core plugs. However, further investigations are required to determine the dependency of the parameters, „a” and „b”, on the injection rate. Using the above derived linear equations along with the Leverett and the analytical relative permeability functions such as those given by Tóth [12] may provide practical convenience and better accuracy in the analysis and interpretation of the immiscible fluid displacement data. The new method presented in this paper offers some advantages for analyzing immiscible fluid displacement data, because it is practical and rapid, and it requires only the conventional coreflow measurements.

NOMENCLATURE

a	empirical constant		
b	empirical constant		
d	core diameter, cm		
f	fractional fluid flow, dimensionless		
L	core length, cm		
N	volume of oil, cm ³		
p	pressure, bar		
Δp	pressure difference, bar		
q	flow rate, cm ³ /s		
S	saturation, dimensionless		
t	time, s		
V	volume, cm ³		
W	volume of water, cm ³		
x	length, cm		
		Subscripts	
		a	breakthrough
		d	displacing
		df	displacing front
		d0	initial displacing
		f	front
		i	injected
		k	displaced
		o	oil
		p	pore or produced
		w	water
			Superscripts
		-	average over core length
		'	denotes a derivative

ACKNOWLEDGEMENT

The authors gratefully acknowledge the Hungarian Scientific Research Fund (OTKA) for support of this work under the contract no. T014890.

REFERENCES

1. Leverett, M.C.: Capillary behavior in porous solids. Trans., AIME (1941) 142, 152-169.
 2. Buckley, S.E. and Leverett, M.C.: Mechanism of fluid displacement in sands. Trans., AIME (1942) 146, 107-116.
 3. Welge, H.J.: A simplified method for computing oil recovery by gas or water drive. Trans., AIME (1952) 195, 91-98.
 4. Sigmund, P.M., McCaffery, F.G.: An improved unsteady-state procedure for determining the relative permeability characteristics of heterogeneous porous media. SPEJ (1979) Febr., 15-28.
 5. Johnson, E. F., Bossler, D.P., and Naumann, V.O.: Calculation of relative permeability from displacement experiments. Trans., AIME (1959) 216, 370-372.
 6. Civan, F., Donaldson, E.C.: Relative permeability from unsteady-state displacements with capillary pressure included. SPE Formation Evaluation (1989) June, 189-193.
 7. Tóth J.: A relatív permeabilitás-görbe számítása a kiszorítási folyamat mérési adataiból. Kőolaj és Földgáz (1982) 15(115), 4 102-105.
 8. Odeh, A.S., Dotson, B.J.: A method for reducing the rate effect on oil and water relative permeabilities calculated from dynamic displacement data. JPT (1985) Nov. 2051-2058.
 9. Islam, M.R., Bentsen, R.G.: A dynamic method for measuring relative permeability. J. Can. Pet. Tech. (1986) Jan.-Febr., 39-50.
 10. Batyky, J.P., McCaffery, F.G., Hodgins, P.K., Fisher, D.B.: Interpreting relative permeability and wettability from unsteady-state displacement measurements. SPEJ (1981) June, 296-308.
 11. Jones, S.C. and Roszelle, W.O.: Graphical techniques for determining relative permeability from displacement experiments. JPT (1978) May, 807-817.
-

12. Tóth J.: Determination of the Leverett- and relative permeability functions from waterflood experiments. *Kőolaj és Földgáz* (1995) 28(128), 3 65-71.
13. Craig, Jr. F.F.: The reservoir engineering aspects of waterflooding. SPE of AIME, New York-Dallas (1971).
14. Shen, C. and Ruth, D.W.: Impact of Inlet Boundary Conditions on the Numerical Simulation of One-Dimensional Coreflooding, *JCPT*, (January 1996), 35 (1), 19-24.
15. Ucan, S., Civan, F. and Evans, R.D.: Uniqueness and Simultaneous Predictability of Relative Permeability and Capillary Pressure by Discrete and Continuous Means, *JCPT*, (April 1997) 36, (4), 52-61.

APPENDIX

REPRESENTATION OF THE FLUID SATURATION DISTRIBUTION ALONG THE CORE PLUG

The objective is to represent the fluid saturation distribution along the core length with a reasonable accuracy based on the information of the saturations at the inlet and outlet faces and the average saturation over the core length. The formulation of the practical interpretation method for analysis of immiscible displacement in laboratory cores presented in this paper is based on the consideration that it will be applied at and after breakthrough. Therefore, it is assumed and verified by experimental data that the saturation distribution of the injected fluid can be adequately represented by the quadratic functions given in the following derivation.

1. Representing the oil saturation distribution during oil injection

Consider a core fully saturated initially with water, thus $S_{w0}=1$. The core is assumed homogeneous and isotropic. During the oil injection, only water is produced until the breakthrough time, t_a . At breakthrough, the oil saturation at the outlet face is S_{of} . The oil saturation at the inlet face is S_{omax} . Let the average oil saturation of the core be \overline{S}_{of} at the breakthrough time.

After breakthrough, $t > t_a$, the oil saturation is S_{omax} at the core inlet, $x=0$ as the volume of the injected oil is infinite compared to the pore volume at that point. Thus, the oil saturation is maximum and only irreducible water saturation ($S_{wi}=1-S_{omax}$) exists at the inlet face. The oil saturation at the outlet face is denoted by S_{o2} . The average oil saturation of the core is \overline{S}_o . Based on the present measurements and experiments, the oil saturation distribution over the core length, L , at a given time, t , can be represented by the following function:

$$S_o(x) = \left(\frac{A}{\frac{x}{L} + B} \right)^2 \quad (A1)$$

The validity of Eq. A1 is confirmed by the cases presented in the applications.

Applying the boundary conditions at the breakthrough time, $t=t_a$, that $S_o(0)=S_{omax}$ at $x=0$, and $S_o(L)=S_{of}$ at $x=L$, the parameters, A and B , are given by the following expressions, respectively:

$$A = \frac{\sqrt{S_{o\max} S_{of}}}{\sqrt{S_{o\max}} - \sqrt{S_{of}}}; \quad (\text{A2})$$

$$B = \frac{\sqrt{S_{of}}}{\sqrt{S_{o\max}} - \sqrt{S_{of}}}. \quad (\text{A3})$$

After breakthrough, $t > t_a$, $S_o(0) = S_{o\max}$ at $x=0$, and $S_o(L) = S_{o2}$. Then, the following expressions are obtained for the parameters:

$$A = \frac{\sqrt{S_{o\max} S_{o2}}}{\sqrt{S_{o\max}} - \sqrt{S_{o2}}}; \quad (\text{A4})$$

$$B = \frac{\sqrt{S_{o2}}}{\sqrt{S_{o\max}} - \sqrt{S_{o2}}}. \quad (\text{A5})$$

For example, if at breakthrough $t = t_a$, $S_{o\max} = 0.81$, $S_{of} = 0.49$ for the oil injection process, then, it is determined that $A = 3.15$, $B = 3.50$ and $\overline{S_o} = 0.6300$, and, therefore, the oil saturation distribution function is estimated to be:

$$S_o(x) = \left(\frac{3.15}{\frac{x}{L} + 3.50} \right)^2, \quad (\text{A6})$$

If at a time after breakthrough $t > t_a$, $S_{o\max} = 0.81$ and $S_{o2} = 0.64$, then it is determined that $\overline{S_o} = 0.7200$, .. $A = 7.20$ and $B = 8$, and the oil saturation distribution function is given by:

$$S_o(x) = \left(\frac{7.20}{\frac{x}{L} + 8} \right)^2. \quad (\text{A7})$$

The average oil saturation over the core length can be estimated using the oil saturation distribution function given by Eq. A1 after breakthrough for $t > t_a$ times:

$$\overline{S_o} = \sqrt{S_{o\max} S_o(x=L)} = \sqrt{S_{o\max} S_{o2}}. \quad (\text{A8})$$

At breakthrough, $t = t_a$, the average oil saturation over the core length is given by:

$$\overline{S_{of}} = \sqrt{S_{o\max} S_{of}}. \quad (\text{A9})$$

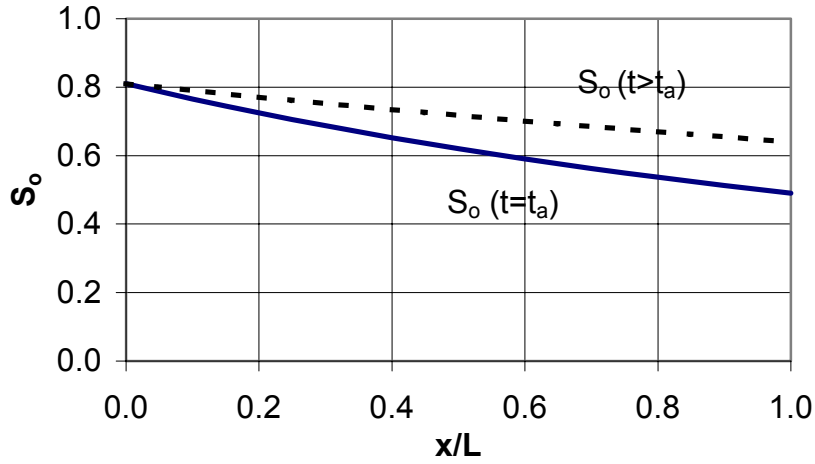


Fig. A1. Saturation distribution during oil injection.

Both Eq. A8 and Eq. A9 imply that the average saturation is equal to the geometric mean of the saturation values at the inlet and outlet faces. Typical saturation distribution and average saturation plots based on the Eqs. A6-A9 are presented in Fig. A1 and A3.

2. Representing the water saturation distribution during water injection

At the beginning of the water injection process, the water saturation in the core is at least equal to the irreducible water saturation S_{wi} or somewhat higher (S_{w0}). After the breakthrough time ($t \geq t_a$), the water saturation distribution along the core can be represented as:

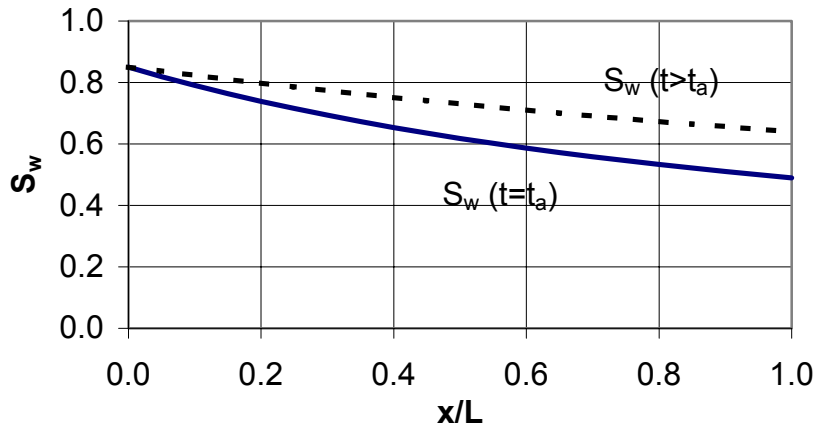


Fig. A2. Saturation distribution during water injection.

$$S_w(x) = S_{w0} + \left(\frac{A}{\frac{x}{L} + B} \right)^2. \quad (\text{A10})$$

Again, the parameters, A and B, are determined by applying the boundary conditions at a given time. At $x=0$, $S_w=S_{max}$, and at $x=L$ $S_w=S_{wf}$ at the breakthrough time $t=t_a$. Thus,

$$A = \frac{\sqrt{(S_{wmax} - S_{w0})(S_{wf} - S_{w0})}}{\sqrt{(S_{wmax} - S_{w0})} - \sqrt{(S_{wf} - S_{w0})}}; \quad (\text{A11})$$

$$B = \frac{\sqrt{(S_{wf} - S_{w0})}}{\sqrt{(S_{wmax} - S_{w0})} - \sqrt{(S_{wf} - S_{w0})}}; \quad (\text{A12})$$

$$\overline{S_{wf}} = S_{w0} + \sqrt{(S_{wmax} - S_{w0})(S_{wf} - S_{w0})}. \quad (\text{A13})$$

After the breakthrough time $t > t_a$ $S_w = S_{w2}$ and therefore:

$$A = \frac{\sqrt{(S_{w2} - S_{w0})(S_{wmax} - S_{w0})}}{\sqrt{(S_{wmax} - S_{w0})} - \sqrt{(S_{w2} - S_{w0})}}; \quad (\text{A14})$$

$$B = \frac{\sqrt{(S_{w2} - S_{w0})}}{\sqrt{(S_{wmax} - S_{w0})} - \sqrt{(S_{w2} - S_{w0})}}; \quad (\text{A15})$$

$$\overline{S_w} = S_{w0} + \sqrt{(S_{wmax} - S_{w0})(S_{w2} - S_{w0})}. \quad (\text{A16})$$

Eqs. A13 and A16 express the average water saturation increment as the geometric mean of the water saturation increments at the inlet and outlet faces.

For example, if the parameters used for water injection are $S_{wmax}=0.85$, $S_{wf}=0.49$, $S_{w0}=0.19$, then:

$$S_w(x) = 0.19 + \left(\frac{1.681163}{\frac{x}{L} + 2.069368} \right)^2. \quad (\text{A17})$$

The core length average water saturation at breakthrough is given as $\overline{S_{wf}} = 0.6350$, and if $S_{wmax}=0.85$, $S_{w2}=0.64$, $S_{w0}=0.19$, then it follows that

$$S_w(x) = 0.19 + \left(\frac{3.849154}{\frac{x}{L} + 4.7380} \right)^2 \quad (\text{A18})$$

and $\overline{S_w} = 0.7350$.

The water saturation distributions calculated by Eqs. A17 and A18 are presented in Fig. A2 and A3. Tables A1 and A2 present comparisons of the published measured data [11], [13] and the data calculated using the above derived relationships. The fact that the average deviation is less than 5 thousandths proves the validity of the theory presented here. This indicates that the average saturation can be calculated using only the saturation values at the inlet and outlet faces. But, in practice, the determination of the saturation at the outlet face is rather difficult. However, note that the average saturation can be readily obtained alternatively using Eq. 13. Therefore, one of the practical advantages of the above described theory is that the saturation value at the outlet face can be estimated at any time during the immiscible displacement by using only the information on the average saturation over the core and the maximum saturation at the inlet face.

Generally, after the breakthrough time, the saturation distribution of the injected fluid along the core can be represented by:

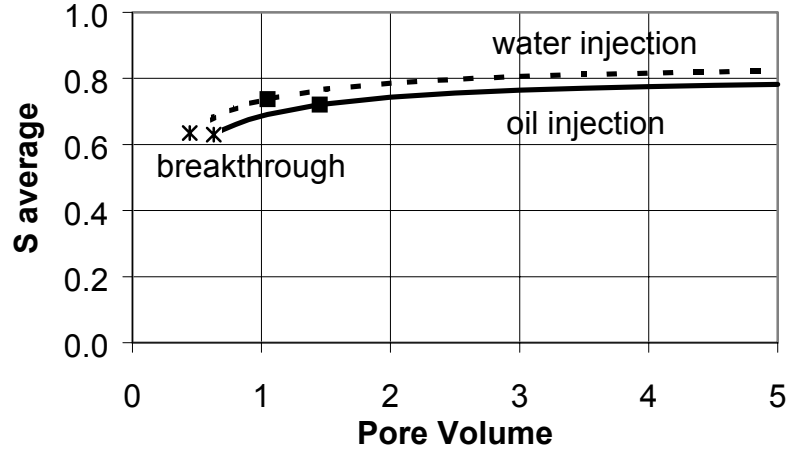


Fig. A3. Average saturation during displacement.

$$S_d = S_{d0} + \left(\frac{A}{\frac{x}{L} + B} \right)^2 . \quad (\text{A19})$$

Then, the average saturation can be expressed in the following manner:

$$\bar{S}_d = \frac{1}{L} \int_0^L \left[S_{d0} + \left(\frac{A}{\frac{x}{L} + B} \right)^2 \right] dx . \quad (\text{A20})$$

From Eq. A20, it can be obtained that:

$$S_{d2} - S_{d0} = b(\bar{S}_d - S_{d0})^2 , \text{ where } b = \left(\frac{B}{A} \right)^2 . \quad (\text{A21})$$

Table A1.

Comparison of the published laboratory data and the calculated data using the present theory.

$S_{wi}=0.35$	$S_{wmax}=0.687$	$S_{wmax}-S_{wi}=0.337$	
\bar{S}_w	S_{w2} (measured)	S_{w2} (calculated)	ΔS_{w2} (meas.-calc.)
0.575	0.511	0.500	+0.011
0.593	0.534	0.525	+0.009
0.627	0.580	0.578	+0.002
0.643	0.617	0.605	+0.012
0.664	0.646	0.643	+0.003
0.675	0.664	0.663	+0.001
0.681	0.676	0.675	+0.001
0.687	0.687	0.687	0
			+0.039/8=+0.00487

Table A2.

Comparison of the published laboratory data and
the calculated data using the present theory.

$S_{wi}=0.10$	$S_{wmax}=0.70$	$S_{wmax}-S_{wi}=0.60$	
$\overline{S_w}$	S_{w2} (measured)	S_{w2} (calculated)	ΔS_{w2} (meas.-cal.)
0.563	0.469	0.457	+0.012
0.582	0.495	0.487	+0.008
0.600	0.520	0.517	+0.003
0.617	0.546	0.546	0
0.636	0.572	0.579	-0.007
0.652	0.597	0.608	-0.011
0.666	0.622	0.634	-0.012
0.681	0.649	0.663	-0.014
0.694	0.674	0.688	-0.014
0.700	0.700	0.700	0
			-0.035/10=-0.0035